Energy-Driven Asymmetric Partitioning of a Semiflexible Polymer between Interconnected Cavities

ARTICLE *in* THE JOURNAL OF PHYSICAL CHEMISTRY B · AUGUST 2008

Impact Factor: 3.3 · DOI: 10.1021/jp801782p · Source: PubMed

3 AUTHORS, INCLUDING:

Peter Cifra
Slovak Academy of Sciences
96 PUBLICATIONS **1,025** CITATIONS
SEE PROFILE

Erik Nies
University of Leuven
78 PUBLICATIONS **951** CITATIONS
SEE PROFILE

Energy-Driven Asymmetric Partitioning of a Semiflexible Polymer between Interconnected Cavities

Peter Cifra,*,† Per Linse,‡ and Erik Nies§

Polymer Institute, Slovak Academy of Sciences, Dúbravská cesta 9, 84236 Bratislava, Slovakia, Physical Chemistry 1, Lund University, Box 124, SE-221 00 Lund, Sweden, Division of Molecular and Nanomaterials, Department of Chemistry, Katholieke Universiteit Leuven, Celestijnenlaan 200F, B-3001 Leuven, Belgium, and Laboratory of Polymer Technology, Eindhoven University of Technology, P.O. Box 513, 5600MB Eindhoven, The Netherlands

Received: February 29, 2008; Revised Manuscript Received: May 9, 2008

The distribution of a semiflexible chain in the volume of two interconnected spherical cavities of equal size has been investigated by using Monte Carlo simulations. The chain possessed an extension exceeding that of the cavity, leading to large probabilities of translocated states despite the entropic penalty of passing the narrow passage. Furthermore, an asymmetric state with unequal subchain lengths in the two cavities was more favorable than the symmetric state. The preference for the asymmetric state is driven by the bending energy. Basically, in the symmetric state both subchains are forced to be bent, whereas in the asymmetric case only one of the subchains must bend, leading to an overall smaller bending penalty and overall smaller free energy of the asymmetric state. These results are in contrast to the entropy-controlled partitioning of polymers into confinement and the symmetric translocation state appearing for flexible polymers.

Introduction

The behavior of biomacromolecules in confined geometries is essential to many biological processes. One of many examples is the packing of semiflexible polymers such as DNA or RNA in viral capsids and their ejection from it.[1,2] Encapsidated polyelectrolytes are subjected to high stress with strong energetic and entropic penalties. Such systems have recently attracted considerable experimental, [3–6] theoretical,[7–10] and simulation[11–14] attention. Important is also the translocation during the chain ejection from the capsid or similar driven translocation through protein channels. The interest in translocation studies was initiated by Kasianovicz et al.[15] and was followed by that in theoretical[16] and simulation[17] studies.

Recent experiments with biopolymers employing fluidic nanochannels constitute another example of confined semiflexible polymers. Such experiments are performed to analyze and understand properties such as the mechanism of the elongation of the polymers in the channels. By using entropic traps,[18] separation of polymers based on their masses can be performed and employed in DNA separation devices. Recent developments[19,20] in micro- and nanofluidic devices fabricated by chip lithography provide a new impetus to study the confinement of biopolymers such as DNA, actin filaments, and microtubules. Micro- and nanofabrications are powerful tools to build up channels of precise geometry and of characteristic dimensions on the order of tens or hundreds of nanometers. Statistical properties of biopolymers confined in channels deviate from those of free chains and depend on the strength and geometry of the confinement. The results of such measurements also serve as a basis for comparison with current theories and mesoscale computer simulations on confined polymers.

Biopolymers are generally stiff on a length scale much larger than their monomer size. The underlying effect in the above-mentioned phenomena is the interplay of three characteristic dimensions: the persistence length of the polymer characterizing the chain stiffness, the polymer coil size, and the extent of the confinement (pore size).

The partition coefficient K for polymers between a free solution and small pores is related to the free energy penalty for the chain on entering the confinement according to $\Delta F/kT = -(\ln K)$. For a polymer with N beads and excluded-volume interactions in a slit or channel with width D, the scaling relation $\Delta F/kT \approx ND^{-1/\nu}$ with $\nu = 0.588$ has been derived, applicable for dilute solutions with weak as well as strong confinement.[21,22] The free energy penalty is entirely due to a decrease of chain entropy upon confinement and, hence, depends only on the coil-to-pore size ratio. A similar but modified scaling law applies also for the semidilute concentration regime,[23] where the coil size in the coil-to-pore size ratio is replaced by a concentration-dependent correlation length. There is an indication that this scaling law applies for relatively weak confinement in a modified form also for more rigid chains.[24] Despite the broad scope of this partitioning relation, there are situations in which the partitioning of polymers is not governed by these scaling laws. It should to be mentioned that the scaling relation for the free energy loss due to the confinement of a macromolecule placed in a closed spherical cavity differs from the above relation.[12,25] According to our numerical observation[26] for partitioning between interconnected (opened) cavities in contrast to closed cavities, the original scaling relation for the case of weak confinement appears still satisfactory.

In a previous study one of us observed a preferred asymmetric translocation state for a semiflexible polymer confined in the volume formed by two interconnected spherical cavities of the same size.[27] This observation was rather unexpected, and it indicated that the confinement in this case is not governed exclusively by the coil-to-pore size ratio. Here, we rationalize

† Slovak Academy of Sciences.
‡ Lund University.
§ Katholieke Universiteit Leuven and Eindhoven University of Technology.

10.1021/jp801782p CCC: $40.75
Published on Web 07/03/2008

this observation and demonstrate that the preferred asymmetric translocation state is rather energy than entropy driven. Thus, with semiflexible and rigid chains that are subjected to a substantial bending penalty by the confinement, the energetics may dominate the translocation equilibrium.

Model and Methods

We have used a coarse-grained model, in which a polymer is represented by interacting beads that are connected by effective bonds and the chain flexibility is controlled by a bending potential. Each effective bond mimicks several chemical bonds along the chain backbone. The model is effectively a discretized representation of a wormlike chain (WLC) but includes also nonbonded interactions. The same model has been used to describe chains in interconnected cavities,[27] the chain elasticity,[28] and the confined structure of stiff polymers.[29]

We have employed the finitely extensible nonlinear elastic (FENE) bond potential[30]

$$U_{\text{bond}}(l) = -\kappa(l_{\max} - l_o)^2 \ln\left[1 - \left(\frac{l - l_o}{l_{\max} - l_o}\right)^2\right] \qquad (1)$$

where l denotes the bond length and κ the bond stretching constant. Furthermore, the bond potential becomes zero and attains its minimum value at $l = l_o$ and diverges at $l \to 2l_o - l_{\max}$ and $l \to l_{\max}$. Here, we have used $l_o = 0.7$ and $l_{\max} = 1$, the latter also defining our unit of length. The contour length of a chain is $L_c = (N - 1)\langle l\rangle$, where N is the number of beads and $\langle l\rangle \approx l_o$ the average length of an effective bond. The chain stiffness has been regulated by employing the bending potential[31]

$$U_{\text{bend}}(\theta) = b^*(1 + \cos\theta) \qquad (2)$$

where θ is the valence angle between two consecutive bonds and b^* the bending rigidity constant. A Morse-type potential has been used for the nonbonded interactions between beads.[30] The potential is composed of a short-range repulsive part and an attractive part according to

$$U_{\text{nonbond}}(r) = \varepsilon\{\exp[-2\alpha(r - r_{\min})] - 2\exp[-\alpha(r - r_{\min})]\} \qquad (3)$$

where r is the bead−bead center-to-center separation and ϵ regulates the interaction strength. The potential minimum $-\epsilon$ appears at $r = r_{\min}$. Here, we have used $r_{\min} = 0.8$ and $\alpha = 24$, making the potential negligible at $r \geq 1$ and leading to an effective core radius $\sigma \approx 0.54l_o$.

In this study, we have employed (i) a chain containing $N = 100$ beads, (ii) a bond stretching constant $\kappa/kT = 20$, (iii) a bending rigidity constant $b^*/kT = b = 35$, and (iv) an interaction strength $\varepsilon/kT = 1$. Moreover, we have for simplicity used Boltzmann constant $k = 1$, and unless otherwise stated temperature $T = 1$, which corresponds to good solvent conditions (Θ temperature 0.6).[30] In free space, the chain has a radius of gyration $R_g = 15.9$. According to the elasticity theory of flexible rods, the persistence length P can be expressed as $P = b\langle l\rangle$,[32,33] which recently has been validated.[28] Hence, since $L_c/P \approx 3$, we regard our chain as semiflexible. For comparison, double-stranded DNA has a persistence length $P \approx 50$ nm, and assuming $2\sigma \approx \langle l\rangle = 2.5$ nm (7.4 base pairs), $b = P/\langle l\rangle = 20$ is obtained[13] as compared to $b = 35$ for the even stiffer chain used here.

The chain was confined in the volume formed by two interconnected spherical cavities with radii $D_1 = D_2 = 10$ connected by a round aperture with a radius $W = 2.5$.[27] Hence, the aperture $2W$ is larger than the diameter of a chain segment 2σ but smaller than 2 times the radius of gyration of the chain, $2R_g$. The size of the aperture also characterizes the interpenetration of cavities and determines the center distance of two cavities. The confining boundary of cavities acts on the bead centers; thus, the radius $D^* = D + \sigma$ should be used to specify the volume available for the beads.

Metropolis Monte Carlo (MC) simulations were used to determine static properties of the confined chain. Overall chain reptation and single-bead translational trial moves were employed. The simulation involved up to 1.8×10^8 MC cycles, where each cycle was composed of N blocks, each block composed of one reptation and five single-bead translational trial moves. Estimated uncertainties of ensemble averages are usually within the size of the symbols in the figures.

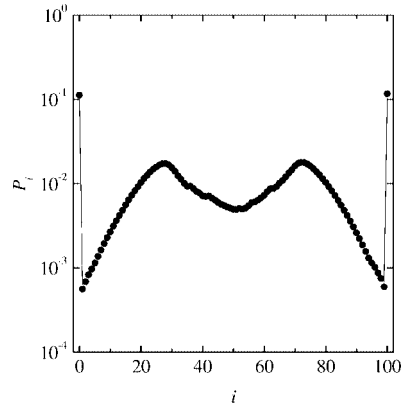

Figure 1. Translocation probability distribution as a function of the number of beads in the second cavity.

Results and Discussion

Central in our study is the location of the chain in the enclosed volume of the two interconnected spherical cavities. We will use the translocation state variable i to describe the number of beads located in cavity 2. Of particular interest is the normalized translocation probability distribution P_i ($i = 0,..., N$) representing the probability of the different states. Specially, P_0 and P_N denote the probability of the states where all beads are in cavities 1 and 2, respectively. By symmetry, we have $P_i = P_{N-i}$.

Figure 1 displays the translocation probability distribution P_i for the present system; similar results were previously given for the same system albeit from a shorter simulation with only reptation trial moves employed.[27] First, the expected mirror symmetry at $i = N/2$ is found, suggesting that the simulation was converged. Furthermore, the following features are noticeable: (i) The probability of finding the chain in one of the cavities is ~20%. As shown later, this relatively high probability is due to the substantial entropy loss when the chain passes through the narrow circular opening connecting the two cavities. (ii) The probability of translocated states increases for small i ($i > 0$) with increasing i, since the chain can better explore the volume of both cavities. (iii) The most probable translocation state (except $i = 0$ and $i = N$) appears at $i \approx 27$ (and $i \approx 73$), and in particular, this asymmetric state is more probable than the symmetric one at $i = 50$. In the following, our main aim is to provide an explanation of why the asymmetric translocation state is more probable than the symmetric one by examination of free energies and their energetic and entropic components.

From the translocation probability distribution P_i, we can obtain the free energy of state i according to

$$F_i/kT = -(\ln P_i) + C \quad (4)$$

where C is yet an unknown constant. Since only free energy differences are of relevance, we form the free energy difference $\Delta F_i = F_i - F_{\text{ref}}$, where F_{ref} is the free energy of a reference state. Two reasonable reference states are possible: (i) an unconfined chain and (ii) the chain confined entirely in one of the cavities, i.e., $i = 0$ (or $i = N$). In the former case, $C - F_{\text{ref}}$ needs to be determined. Since our interest is the distribution of the chain in the confined volume, the second reference state is sufficient and also more convenient. Hence, with $F_{\text{ref}} = F_0$ we have

$$\Delta F_i/kT = F_i/kT - F_0/kT = -(\ln P_i/P_0) \quad (5)$$

where the second equality was obtained by insertion of eq 4. The total potential energy of a given conformation is obtained by summing the bond, bending, and nonbonded potential energies. Furthermore, the internal energy of each translocation state, U_i, was evaluated by averaging the total potential energies after classification of a given conformation into a state. From the set of U_i, the internal energy difference ΔU_i was obtained according to

$$\Delta U_i = U_i - U_0 \quad (6)$$

Similar averaging of the three potential energy contributions over different translocation states was also made. Finally, the entropy difference ΔS_i, expressing the entropy difference between state i and state 0, is given by the thermodynamic relation

$$-\Delta S_i = (\Delta F_i - \Delta U_i)/T \quad (7)$$

Starting with the three potential energy contributions, Figure 2 provides the bond, bending, and nonbonded potential energies for the different states relative to state 0. For completeness, for state 0 we obtained $U_{\text{bond},0} = 34.25kT$, $U_{\text{bending},0} = 110.24kT$, and $U_{\text{nonbonoded},0} = -0.32kT$, making $U_0 = 144.17kT$, which could be compared to the total potential energy of an unconfined chain of $136.02kT$. Figure 2 shows that the bond and nonbonded potential energies hardly vary with the translocation state. On the other hand, the bending potential energy displays a strong dependence on the translational state with variations up to $3kT$.

The free energy difference and its energy and entropy components according to eqs 5–7 are given in Figure 3. The free energy curve provides by construction the same information as given by the translocation probability distribution given in Figure 1. However, we now directly see that (i) the free energy of the asymmetric state is $1.9kT$ above that for the chain in one of the cavities and (ii) the free energy of the symmetric state is an additional $1.3kT$ higher.

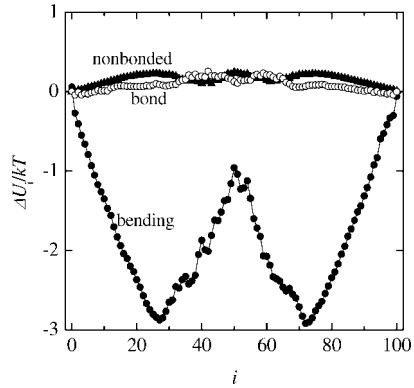

Figure 2. Bond, bending, and nonbonded potential energy difference as a function of the translocation state i.

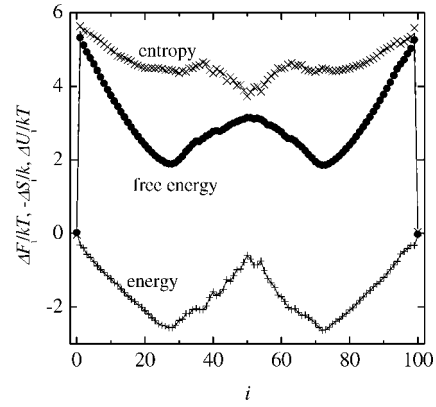

Figure 3. Free energy difference and its energy and entropy components as a function of the translocation state i.

As for the internal energy, we have already found that its dependence on the translocational state depends mainly on the bending potential energy. From Figure 3 we see that the highest internal energy is obtained when the chain is placed entirely in one of the cavities, which is a direct consequence of an extensive degree of chain bending. As the translocation starts and proceeds, the bending potential energy is progressively reduced until $i \approx 27$, which stems from a reduction of the length of the longer and bent subchain, whereas the growing and shorter subchain remains unbent in the second cavity. At $i \approx 27$ the shorter subchain starts to become affected by the confinement, and at a further translocation this subchain must also bend. This results in a local maximum of the bending potential energy for the symmetric state, the maximum being $2.0kT$ above the asymmetric minimum and $0.6kT$ below the energy of the chain confined in one cavity.

Regarding the entropy, there is a large entropy penalty, $5.6k$, for the chain to have one of its two end beads protruding into the small opening between the two cavities. An approximate expression of $\Delta S_1/k$ based on volume arguments only is given in the Appendix. As the translocation proceeds, the entropy penalty decreases and reaches a local minimum for the symmetric state, but it is still $4.4k$ above that for the chain in one cavity. As compared to the asymmetric state, the symmetric one is favored by $0.7k$. The appearance of a local entropy minimum for the symmetric state is natural since the entropy should favor a homogeneous distribution of the beads between the two cavities.

By comparing the energy and entropy profiles in Figure 3, it is clear that the resulting free energy profile is dominated by the energy, and in particular, the favorable asymmetric state is energetically driven. A comparison between the asymmetric and symmetric states shows that the asymmetric state is energetically favored by $2.0kT$ and entropically disfavored by $0.7k$, resulting in an overall free energy preference by $1.3kT$.

On the basis of the thermodynamic analysis, we provide the following simple explanation. Our semiflexible chain becomes compressed when being placed in one of the cavities. In the asymmetric state, the two subchains have different lengths; the shorter one is sufficiently short to attain a stretched configuration and only the longer one is forced to be bent to fit in the cavity. On the other hand, in the symmetric state each subchain has to bend in each of the two cavities. Of course, the chain bending is redistributed along the chain continuously, but this simplified picture seems to hold. Figure 4 provides typical snapshots for the asymmetric and symmetric states supporting this explanation.

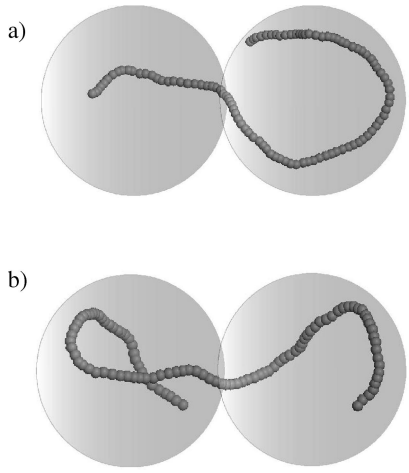

Figure 4. Snapshots of configurations representing the asymmetric (a) and symmetric (b) states.

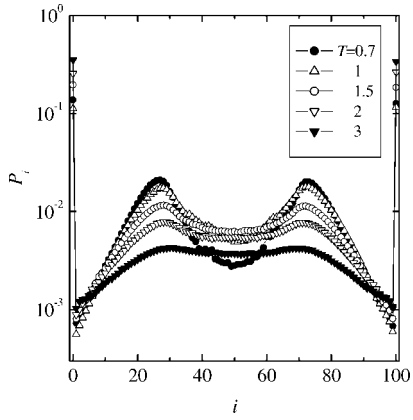

Figure 5. Translocation probability as a function of the number of beads in the second cavity at the reduced temperatures $T = 0.7$, 1, 1.5, 2, and 3.

So far, results have been given at the reduced temperature $T = 1$. Figure 5 displays the translocation probability distribution P_i at reduced temperatures in the range from 0.7 to 3 and confirms the importance of the energy in partitioning obtained above from the free energy decomposition at a single temperature only. We observe that at the highest temperature considered the probabilities of the asymmetric and symmetric states are essentially identical, whereas the asymmetric state is favored upon temperature reduction. At decreasing T the energy contribution to the free energy becomes more important; namely, the chain rigidity increases, which drives the system to the asymmetric translocation, and vice versa, with temperature increasing, the entropy dominates the free energy and the symmetric state is favored. We also notice that the probability of the nontranslocated states ($i = 0$ and $i = N$) decreases as T is reduced from 3 to 1, which originates from a larger energy penalty for the chain being confined in one cavity and a reduced entropic penalty of passing the neck of the two cavities.

We also investigated the behavior of other chain lengths to verify our conclusions. For the same geometry and $T = 1$, the shorter chain, $N = 70$, provided a symmetric translocation distribution as expected (not shown here). For the longer chain, $N = 200$, the distribution exhibited more complex behavior with three maxima: a symmetric peak and two satellite peaks, representing a more complex chain arrangement under strong confinement. To complete the picture, it should be noticed that the crossover to flexible behavior in translocation distributions was shown previously.[27]

Conclusions

In partitioning of polymers into confined spaces such as pores or channels, an entropic driving force is well-established and used to explain most of the observed behavior. This view depends on the fact that the chains are flexible. The present study showed that, for semiflexible chains under confinement, the partitioning between two connected cavities can also be controlled by the internal energy and in particular the bending energy at certain temperatures. Hence, the partitioning is energy-driven in contrast to entropy-driven partitioning of flexible polymers. In other words, not only the coil-to-pore size ratio but also the persistence length and chain contour length come into play in determining the partitioning. The distribution of chain bending over the translocating chain allows for interesting asymmetric equilibrium conformations. This observation should be of relevance for, e.g., the confinement of DNA in small pores.

Acknowledgment. This work was financially supported by VEGA Grant 2/6116/26, Grant APVV-0079-07, in part by the Centre of Excellence COMCHEM, the Flemish Science Foundation, and the Slovak Academy of Sciences in the framework of the bilateral exchange agreement between Flanders and Slovakia, and the Swedish Research Council (VR) through the Linnaeus Center of Excellence on Organizing Molecular Matter (OMM).

Appendix

Consider a chain composed of connected beads separated by the distance a. The chain is confined inside a spherical cavity with radius D, and the cavity possesses a round aperture with radius W. The entropy cost of having *exactly* one of the end beads placed within the aperture (in the main text denoted by ΔS_1) can by volume arguments be estimated as

$$\exp[\Delta S_1/k] \approx 2V_1/V_0 \tag{A1}$$

where V_1 is the volume available for an end segment in the apperture approximated by $V_1 = \pi W^2 a$ and V_0 the volume available for the end segment in the nontranslocated state given by $V_0 = (4\pi/3)D^3$. Insertion of these volume expressions into eq A1 gives

$$\exp[\Delta S_1/k] = \frac{3W^2 a}{2D^3} \tag{A2}$$

We note that the predicted value of ΔS_1 is independent of the chain flexibility and solvent condition.

With the values $D = 10$, $W = 2.5$, and $a = 0.7$ used in the main text, we get $-\Delta S_1/k \approx 5.0$. This should be compared to $-\Delta S_1/k = 5.6$ as obtained from the simulations. Four other comparisons of values of $\Delta S_1/k$ obtained from simulation and eq A2 for the conditions $(D, W) = (12, 2)$, $(8, 3)$, $(7, 3)$, and $(6, 2.5)$ provided a deviation between 3% and 20%. This shows that, at least for these conditions, the main contribution to ΔS_1 most likely can be explained through volume arguments.

References and Notes

(1) Roos, W. H.; Ivanovska, I. L.; Evilevitch, A.; Wuite, G. J. L. *Cell. Mol. Life Sci.*, in press.
(2) Angelescu, D. G.; Linse, P. *Curr. Opin. Colloid Interface Sci.*, in press.
(3) Nykypanchuk, D.; Strey, H. H.; Hoagland, D. A. *Macromolecules* **2005**, *38*, 145–150.
(4) Castelnovo, M.; Evilevitch, A. *Eur. Phys. J. E* **2007**, *24*, 9–18.
(5) Löf, D.; Schillén, K.; Jönsson, B.; Evilevitch, A. *Phys. Rev. E* **2007**, *76*, 011914.

(6) Sikkema, F. D.; Comellas-Aragones, M.; Fokkink, R. G.; Verduin, B. J. M.; Cornelissen, J. J. L. M.; Nolte, R. J. M. *Org. Biol. Chem.* **2007**, *5*, 54–57.

(7) (a) Muthukumar, M. *Phys. Rev. Lett.* **2001**, *86*, 3188–3191. (b) Cacciuto, A.; Luijten, E. *Phys. Rev. Lett.* **2006**, *96*, 238104.

(8) van der Schoot, P.; Bruinsma, R. *Phys. Rev. E* **2005**, *71*, 061928.

(9) Slosar, A.; Podgornik, R. *Europhys. Lett.* **2006**, *75*, 631–637.

(10) Angelescu, D. G; Linse, P; Nguyen, T. T; Bruinsma, R. F *Eur. Phys. J.*, in press.

(11) Pais, A. A. C. C.; Miguel, M. G.; Linse, P.; Lindman, B. *J. Chem. Phys.* **2002**, *117*, 1385–1394.

(12) Luijten, E.; Cacciuto, A. *Nano Lett.* **2006**, *6*, 901–905.

(13) Ali, I.; Marenduzzo, D.; Yeomans, J. M. *Phys. Rev. Lett.* **2006**, *96*, 208102.

(14) Angelescu, D. G.; Bruinsma, R.; Linse, P. *Phys. Rev. E* **2006**, *73*, 041921.

(15) Kasianowics, J. J; Brandin, E; Branton D; Deaner, D. W. *Proc. Natl. Acad. Sci. U.S.A.* **1996**, *93*, 13770–13779.

(16) Kong, C. Y.; Muthukumar, M. *J. Chem. Phys.* **2004**, *120*, 3460–3466.

(17) Sousa, A. F.; Pais, A. A. C. C.; Linse, P. *J. Chem. Phys.,* **2005**, *122*, 214902.

(18) Han, J; Craighead, H *Science* **2000**, *288*, 1026–1029.

(19) Tegenfeldt, J. O.; Prinz, C.; Cao, H.; Chou, S.; Reisner, W. W.; Riehn, R.; Wang, Y. M.; Cox, E. C.; Sturm, J. C.; Silberzan, P.; Austin, R. H. *Proc. Natl. Acad. Sci. U. S. A.* **2004**, *101*, 10979–10983.

(20) Reisner, W. W.; Morton, K. J.; Riehn, R.; Wang, Y. M.; Yu, Z.; Rosen, M.; Sturm, J. C.; Chou, S. Y.; Frey, E.; Austin, R. H. *Phys. Rev. Lett.* **2005**, *94*, 196101.

(21) Casassa, E. F. *J. Polym. Sci., Polym. Lett. Ed.* **1967**, *5*, 773.

(22) Daoud, M.; de ennes, P. G. *J. Phys. (Paris)* **1977**, *38*, 85–93.

(23) Wang, Y.; Teraoka, I. *Macromolecules* **1997**, *30*, 8473–8477.

(24) Škrinárová, Z; Cifra, P. *Macromol. Theory Simul.* **2001**, *10*, 523–531.

(25) Grosberg, A. Y.; Khokhlov, A. R. *Statistical Physics of Macromolecules*; American Institute of Physics: New York, 1994.

(26) Cifra, P. *Macromolecules* **2005**, *38*, 3984–3989.

(27) Cifra, P. *J. Chem. Phys.* **2006**, *124*, 024706.

(28) Cifra, P.; Bleha, T. *Polymer* **2007**, *48*, 2444–2452.

(29) Cifra, P.; Benková, Z.; Bleha, T. *J. Phys. Chem. B* **2008**, *112*, 1367–75.

(30) Milchev, A.; Binder, K. *Macromolecules* **1996**, *29*, 343–354.

(31) Fynewever, H.; Yethiraj, A. *J. Chem. Phys.* **1998**, *108*, 1636–1644.

(32) Yamakawa, H. *Modern Theory of Polymer Solutions*; Harper & Row: New York, 1971.

(33) Hakansson, C.; Elvingson, C. *Macromolecules* **1994**, *27*, 3843–3849.

JP801782P